02

Resonance of a thin film phonon with the surface polariton of the substrate

© V.A. Yakovlev, N.N. Novikova, S.A. Klimin¶

Institute of Spectroscopy, Russian Academy of Sciences, Troitsk, Moscow, Russia

¶e-mail: klimin@isan.troitsk.ru

Received June 07, 2024
Revised June 07, 2024
Accepted July 29072024

In layered structures, optical effects are, as a rule, linear across film thicknesses (at small thicknesses). Therefore, theoretically predicted by V.M. Agranovich, the root dependence of surface polariton (SP) splitting on thickness is unique. This work demonstrates the splitting of the sapphire SP dispersion curve after deposition of a magnesium oxide film on its surface. The magnitude of this splitting is proportional to the square root of the transition layer thickness, as predicted by theory. A review of other experiments confirming the theoretical conclusions is carried out.

Keywords: surface phonon polaritons, ATR spectroscopy, thin films, dispersion analysis, dispersion curves, magnesium oxide, sapphire.

DOI: 10.61011/EOS.2024.08.60023.6792-24

1. Introduction

This study will discuss the experimental validation of a theoretically predicted splitting of a substrate's surface polariton (SP) in the presence of a nanometer-thick transition layer. The effect was predicted in 1974 in „Surface Polaritons in Resonance with Transition Layer Vibrations" [1] by V.M. Agranovich and A.G. Mal'shukov. Later, V.M. Agranovish published review [2] focused on SP crystal optics and surface properties. Figure $1, a$ [2] shows that there is a domain of SP existence in the spectral interval between the transverse (TO, $\Omega_{\perp}$) and longitudinal (LO, $\Omega_{\parallel}$) frequencies of the crystal phonon. Figure $1, b$ shows that when there is a transition layer on the crystal surface, then SP is split when the transition layer frequency (ω_0) is in resonance with the polariton (Figure $1, b$). In [1], it was shown that the magnitude of splitting is directly proportional to the square root of transition layer thickness. This allows researchers to study optical properties of thin film coatings even of a nanometer range using the SP spectroscopy.

In recent decades, nanometer-thick films have been widely used in micro-/optoelectronic applications. Functional thin films are usually deposited on a substrate to ensure adequate strength and durability. Due to the lattice mismatch of two materials, properties of films on substrates may be much different from those of bulk materials from which they are fabricated, which certainly necessitates the study of their properties to further elaborate the technologies of coatings with pre-defined properties. However, the existing traditional optical spectral methods using reflection and transmission spectra are insufficiently sensitive to ultrathin films because, due to their low optical density, the films are not visible in the infrared (IR) transmission and reflection spectra against the background of the substrate spectra. In this case, good results for determining the physical parameters of nanofilms are provided by the SP spectroscopy developed by distinguished physicist V.M. Agranovich.

SPs are defined as waves propagating along a media interface provided that permittivities of the media in contact are of different signs. The field of these waves is maximum at the interface and decreases exponentially with distance [3,4] when moving from the interface (Figure $2, a$). Such (near) field is the advantage of the SP spectroscopy compared with traditional methods of study of nanoscale objects.

The theoretical prediction of [1] was supported experimentally in [5–7]. Using the SP spectroscopy, a resonance of the longitudinal phonon of the LiF (film) transition layer with SP of the Al_2O_3 (sapphire) substrate was observed. SP dispersion curve splitting was observed in the spectra. The magnitude of splitting followed the root dependence of the film thickness. Experimental evidence of the predictions in [1] was later also obtained for other film/substrate systems [8–17]. SP splitting was also observed on transition layers occurring due to crystal surface modification [18,19].

This work elaborates MgO thin film coatings grown on sapphire substrates. Results obtained using the „traditional" „external" reflection spectroscopy and the attenuated total reflection (ATR) spectroscopy methods were compared. It is shown that the MgO phonon, whose longitudinal vibration frequency gets into resonance with sapphire's SP, splits the dispersion curve of the latter. It is shown that substrate SP splitting is proportional to the square root of film thickness as predicted in [1]. Finally, the experimental data existing in the literature is compared for various resonance cases.

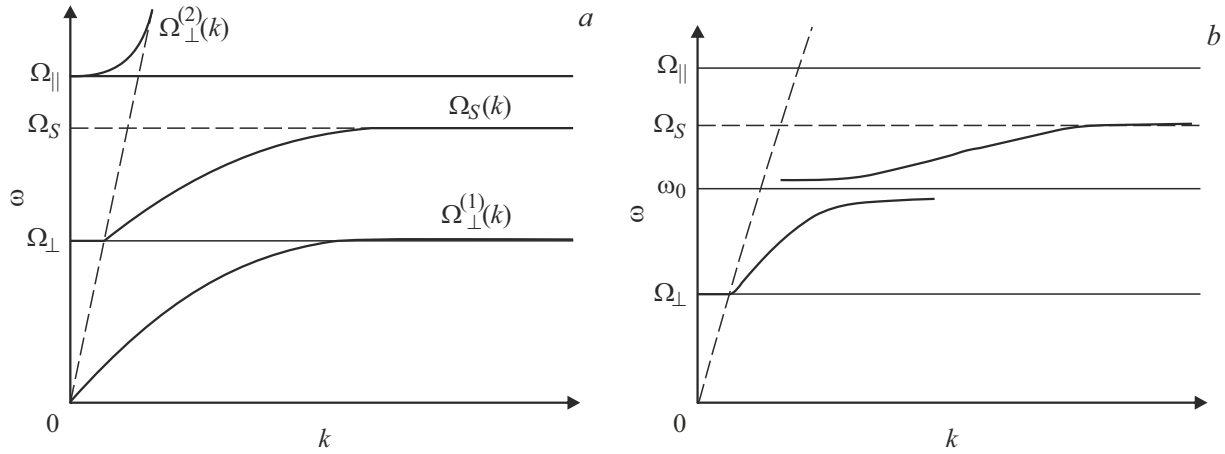

Figure 1. (*a*) Polariton dispersion for the planar media interface. (*b*) Polariton dispersion in the presence of resonance with transition layer vibrations. The pictures are taken from V.M. Agranovich's work [2].

2. Experiment details

The experiment examined four samples of MgO thin films on the (0001) plane of single-crystal sapphire (α-Al_2O_3) having a thickness of about 1 mm. The films were grown using the vapor-phase deposition method [20] at the Institute of Inorganic Chemistry and Surfaces, Padova, Italy, The MgO film thickness was 300, 100, 30 and 10 nm.

IR reflection and ATR spectra were measured using the Bruker IFS 66 v/s Fourier transform spectrometer at room temperature in a spectral range from 450 to 5000 cm^{-1}. External reflection was examined with near-normal light incidence. The middle IR ATR spectra with a resolution of 4 cm^{-1} in the *p*-polarized light were measured in the Otto configuration [21] (Figure 2, *b*) using a KRS-5 prism with variation of the light incidence angle θ in a range from 26° to 63°, i.e. at angles larger than the critical angle of total internal reflection (25°) defined by condition through the refraction index of KRS-5 $\sin\vartheta_{cr} = 1/n_{KRS-5}$.

ATR spectra are very sensitive to the thickness of a gap between the sample and prism because the prism perturbs the SP field. For correct measurement of the SP absorption frequency and bandwidth at various light incidence angles in the prism, such gap thickness was selected at which the intensity of the measured band was of the order of few percent. In this case, SP perturbation by the prism is not too high. Air gap between the prism and sample was varied from several microns to tens of microns using mylar spacers. Frequency-angle dependence of SP was measured. SP dispersion curves were plotted from the angular dependence of the ATR spectra.

3. Results and discussion

3.1. External reflection spectra of the MgO films on sapphire

Figure 3, *b, c* shows the external IR reflection spectra for the 10, 30, 100, 300 nm MgO films on sapphire substrates and the substrate spectrum (for comparison). The reflection spectra for two samples with the thinnest films almost retrace the substrate reflection spectrum. At the same time, the samples with 100 and 300 nm films exhibit changes in a low-frequency region in the vicinity of 400 cm^{-1}.

Parameters of the IR-active vibrational modes of the E_u symmetry of the Al_2O_3 substrate: transverse and longitudinal vibration frequencies ν_{TO} and ν_{LO}, oscillator strengths $\Delta\varepsilon$ and decay constants γ. $\varepsilon_\infty = 3.15$

Designation	ν_{TO}, cm^{-1}	ν_{LO}, cm^{-1}	$\Delta\varepsilon$	γ, cm^{-1}
E_u^1	384.8	387	0.27	4.9
E_u^2	440	483	3.01	2.2
E_u^3	565.4	908	3.21	19
E_u^4	633	629	0.13	4.8

IR-active phonons of sapphire (α-Al_2O_3) are well studied [23–25]. The measured reflection spectra for the substrate with the (0001) orientation agree with the existing literature data. The Al_2O_3 crystal is uniaxial and crystallizes in the trigonal crystal system, space group $R3c$ [26,27]. The spectrum in Figure 2, *b* exhibits (in accordance with the selection rules) four Eu symmetry phonons. Dialectric function of the sapphire was calculated using the reflection spectrum dispersion analysis method in SCOUT [28,29] and RefFIT software [30]. The reflection coefficient $R(\nu)$ was calculated using the Fresnel equations for reflection of light from laminar structures. The complex dialectric function ε was expressed through a sum of contributions of N (four for sapphires) damped oscillators:

$$\varepsilon(\nu) = \varepsilon_1 + i\varepsilon_2 = \varepsilon_\infty + \sum_{j=1}^{N} \Delta\varepsilon_j \frac{\nu_{TOj}^2}{\nu_{TOj}^2 - \nu^2 + i\gamma_j\nu}. \quad (1)$$

Here ν_{TOj}, $\Delta\varepsilon_j$ and γ_j are the transverse oscillation (TO) frequency, oscillator strength and damping constant

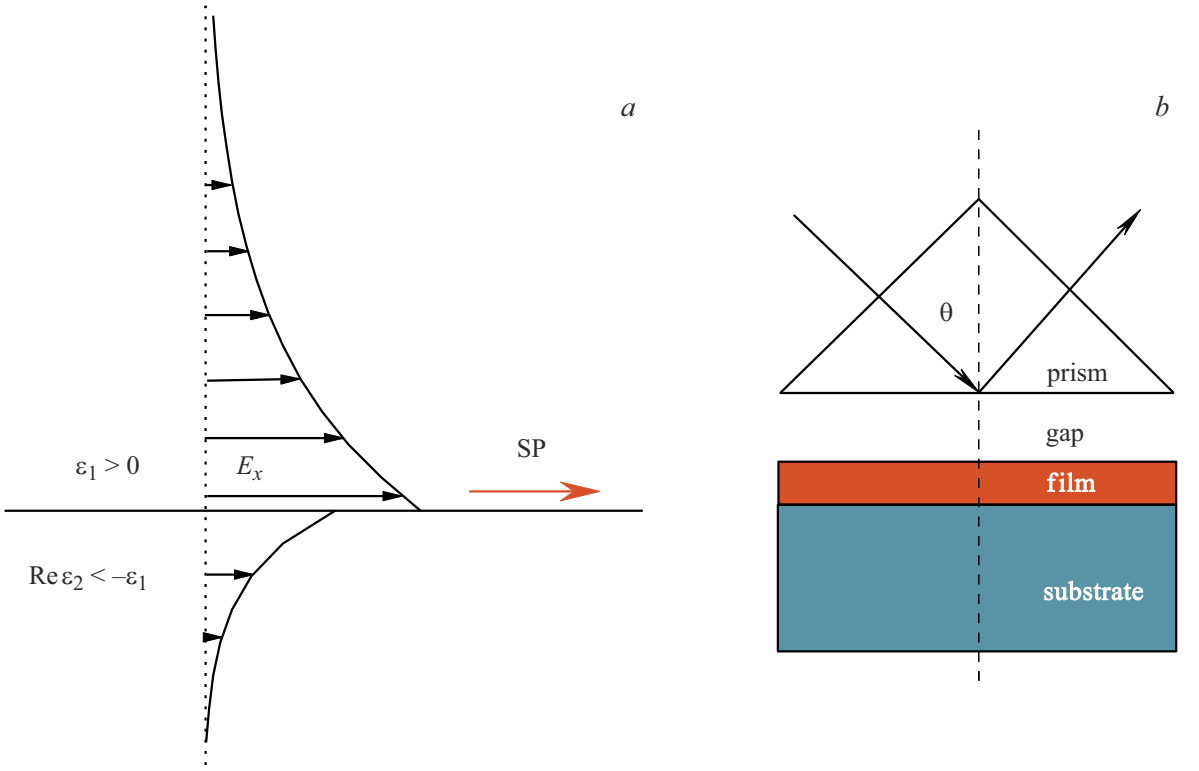

Figure 2. *a*) Schematic diagram of the electromagnetic field of SP and its excitation condition. (*b*) SP excitation in the Otto configuration.

of the jth phonon, respectively; ε_∞ is the high-frequency permittivity, ε_1 and ε_2 are the real and imaginary parts of ε.

Optical parameters obtained by fitting the sapphire reflection spectrum are listed in the table. The phonon E_u^4 is inverted [31–37]. This is a weak phonon whose frequency got into the TO–LO-splitting of the strong phonon E_u^3. Its TO- and LO-frequencies are inverted: $\nu_{\mathrm{TO}} > \nu_{\mathrm{LO}}$. On the reflection spectrum, it looks like an absorption line in the high reflection region (reststrahlen region).

The resulting dependence $\varepsilon_1(\nu)$ is shown in Figure 3, *a*. The region of negative values of ε_1 is marked by a grey bar at the top of the figure. This region begins a little higher in frequency than the TO frequency $\nu_{\mathrm{TO}} = 565\,\mathrm{cm}^{-1}$ of the strong phonon E_u^3 and extends almost up to its LO frequency. The presence of a wide spectral region with $\varepsilon_1 < -1$ makes sapphire convenient for the SP spectroscopy.

Vibrational properties of MgO are also well studied [38–41]. The crystal has a cubic symmetry, space group $Fm\bar{3}m$ [42]. One phonon is active in the IR spectra. Its transverse frequency is $\nu_{\mathrm{TO}} = 418\,\mathrm{cm}^{-1}$ [41]. Singularities in the reflection spectra for 100 nm and 300 nm films occur exactly in the vicinity of the TO frequency of the MgO phonon.

The longitudinal frequency of the IR-active MgO phonon is $\nu_{\mathrm{LO}} = 738\,\mathrm{cm}^{-1}$ [41] and falls into the sapphire's SP region. A scheme shown in Figure 1, *b* is implemented. Thus, the study of SP spectra of the MgO/sapphire films is of high interest for verification of the conclusions in [1].

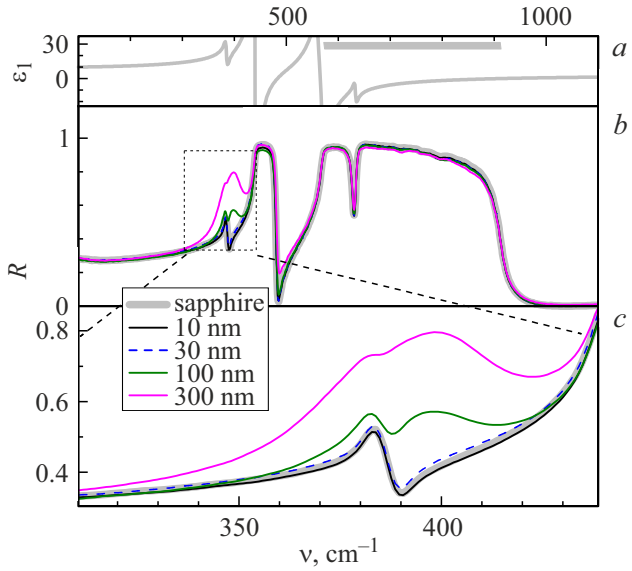

Figure 3. (*a*) Real part of sapphire's dialectric function ε_1. Grey bar corresponds to the region of negative values of ε_1. (*b, c*) Reflection spectra of 10, 30, 100 and 300 nm MgO thin films on substrates compared with the sapphire substrate spectrum.

3.2. SP dispersion on sapphire

Figure 4 shows the color map of the ATR spectra intensities of the sapphire substrate in the frequency - wave vector coordinates. A reduced wave vector (k/k_0) is used,

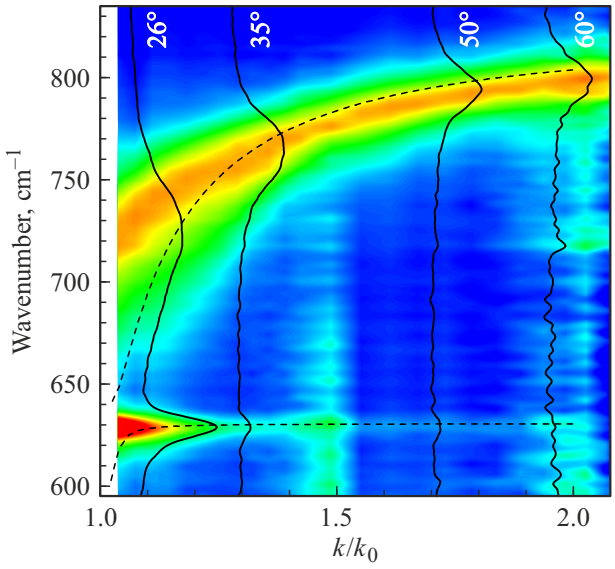

Figure 4. Color map of the sapphire's ATR spectra intensities in the frequency - reduced wave vector coordinates. Four spectra for various light incidence angles (black lines) are shown. Calculated data — dashed lines.

where k_0 is the wave vector at the critical ATR angle (25°). The figure also shows four spectra at the selected wave vectors. Two peaks are observed in the ATR spectra. One of the peaks is at a frequency in the vicinity of 630 cm^{-1}. The frequency of this peak remains almost unchanged when the wave vector varies, and its intensity decreases considerably for high values of k. This absorption peak corresponds to SP resulting from the bound state of the photon and phonon E_u^4. Shift of the corresponding peak depending on k takes place within the SP's TO–LO-splitting which is not too large and is only 4 cm^{-1}.

The second peak in the ATR spectra in Figure 4 shifts considerably (from 725 to 790 cm^{-1}) when k varies. This peak corresponds to SP resulting from the bound state of the photon and phonon E_u^3. For this SP, high dispersion is observed (orange curve on the intensity map Figure 4), SP frequency is between the TO and LO frequencies of the phonon E_u^3.

For comparison, Figure 4 also shows the SP dispersion branch calculation data obtained using the procedure described in [15,43]. Good qualitative agreement between the experiment and calculation is observed. At low values of k, data mismatch grows. It is due to the fact that two SPs interact with each other, this leads to intensity transfer between peaks as well as to quasiparticle repulsion.

3.3. ATR spectroscopy of nanometer-thick MgO films

Figure 5 shows the intensity maps and ATR spectra for the 300, 100, 30 and 10 nm MgO films on sapphire. For the 300 and 100 nm films, the ATR spectra contain three peaks for most wavenumbers, rather than two peaks as in the sapphire case. This suggest that the sapphire's SP dispersion curve is split. Consequently, two SP dispersion branches are observed. The minimum distance for different k between these branches is referred to as splitting Δ (Figure 5, *a*). For the 300 nm film, splitting is the highest and is equal to 105 cm^{-1}, for the 100 nm film - it is equal to 62 cm^{-1}. Figure 6, *a* shows the ATR spectra of all samples with films of different thicknesses at the incidence angle of 26°. It can bee seen that splitting of the line at 720 cm^{-1} grows considerably with an increase in the MgO film thickness. For the 10 nm film, only a weak shoulder is observed on the low-frequency side of the line. The ATR spectrum of the 30 nm film contains a clear splitting of the 720 cm^{-1} line. For the 100 nm film, split lines are at a considerable distance, for the 300 nm film, splitting is so large that the low-frequency component intersects the 620 cm^{-1} line. As shown in Figure 5, *a*, at small incidence angles, further interaction between the two SPs takes place in the vicinity of 620 cm^{-1}.

For the 30 nm and 10 nm MgO films, the intensity maps in Figure 5 do not provide any clear splitting picture. This is due to the small thickness and, consequently, to low intensity of SP resulting from the interaction between light and the MgO phonon. When the frequencies of two SPs approach each other depending on k , their resonance interaction and, as a consequence, intensity transfer occur. As a result, as mentioned above, the ATR spectra of the 30 nm film at the angles within 26°–33° have the absorption line at 670–750 cm^{-1} consisting of two closely-spaced components (see also Figure 6, *a*). Thus, the magnitude of splitting Δ may be estimated and, according to our data, is equal to 30 ± 5 cm^{-1}. For the 10 nm film, only weak shoulders are observed near the main line which also suggest splitting of the polariton dispersion curve. Figure 6, *b* shows how the line shifts in the ATR spectrum of the 30 nm film sample at various values of k. Besides the shift, change in the linewidth is also observed. Figure 6, *c* shows the dependence of FWHM of this line depending on k. A considerable growth of the width at low values of k. This growth is assigned to the sapphire's SP splitting effect. The estimate of Δ for the 10 nm film by the FWHM difference near and far from the resonance gives 17 ± 3 cm^{-1}.

Figure 5 shows the SP dispersion curves calculated using equations [15] for all samples and displayed as dashed lines. Good qualitative agreement between the calculated and experimental curves is observed. The experimental findings described in this section show that the SP spectroscopy can really give good results when investigating thin films with thicknesses up to approximately ten nanometers.

3.4. Dependence of the magnitude of splitting on film thickness

The values obtained in the previous section for Δ for films of different thicknesses are shown in Figure 7 as blue circles.

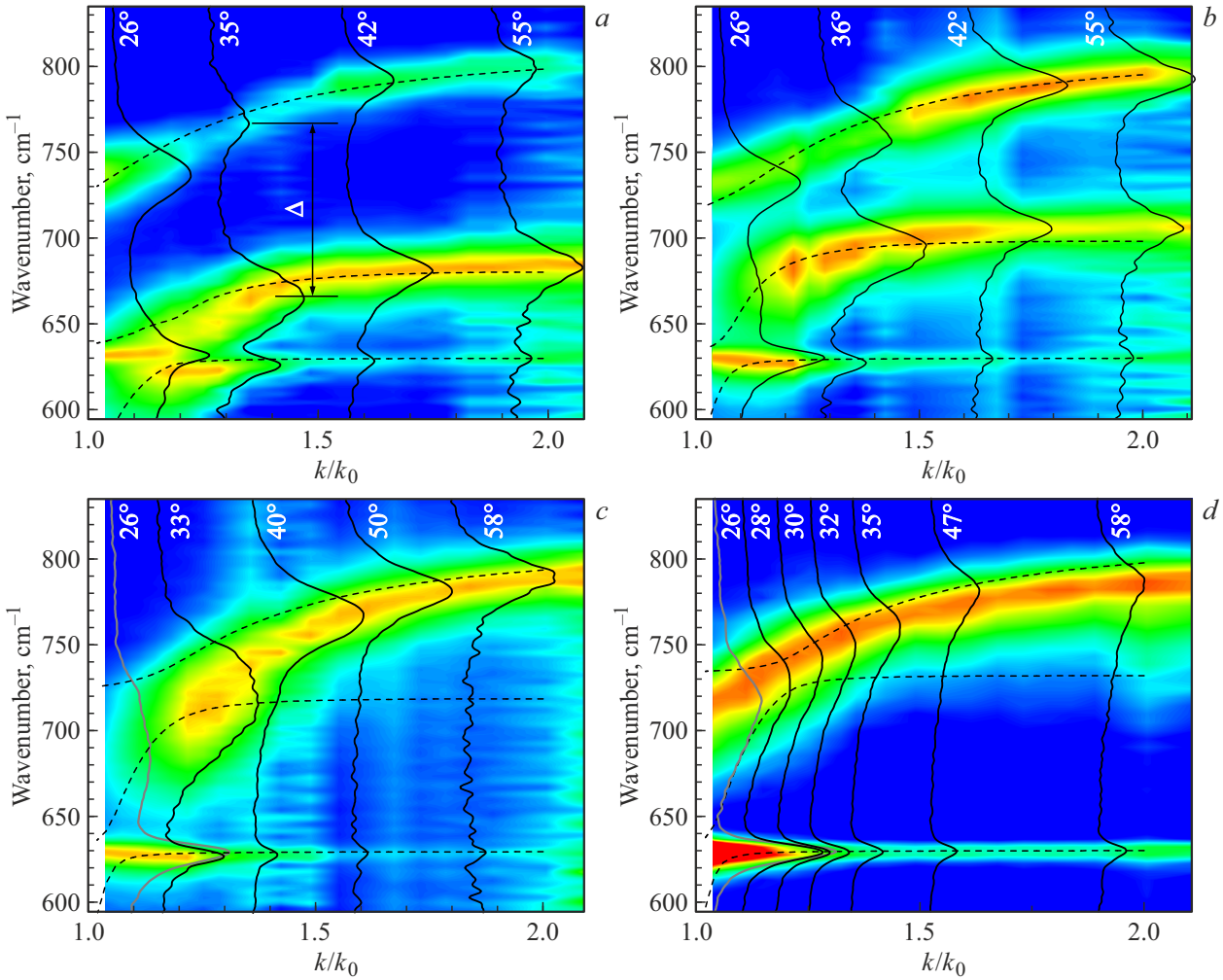

Figure 5. Color maps of the ATR spectra intensities of the MgO films on sapphire substrates in the frequency — reduced wave vector coordinates. MgO film thickness is (*a*) 300 nm, (*b*) 100 nm, (*c*) 30 nm and (*d*) 10 nm. Four spectra for various light incidence angles (black solid lines) are shown. Calculated data — dashed lines.

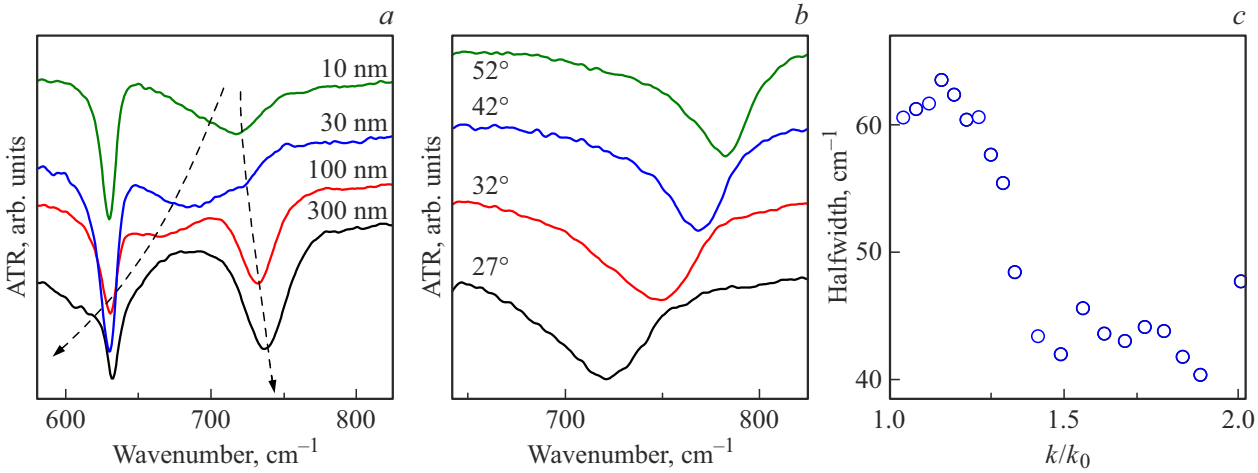

Figure 6. (*a*) ATR spectra of the MgO films of various thicknesses on sapphire for the incidence angle 26°. (*b*) ATR spectra of the 10 nm MgO film on sapphire at various incidence angles. (*c*) Full width at half maximum of the absorption line in the ATR spectra of the 10 nm MgO film for the line shown in Figure *b* depending on the wave vector.

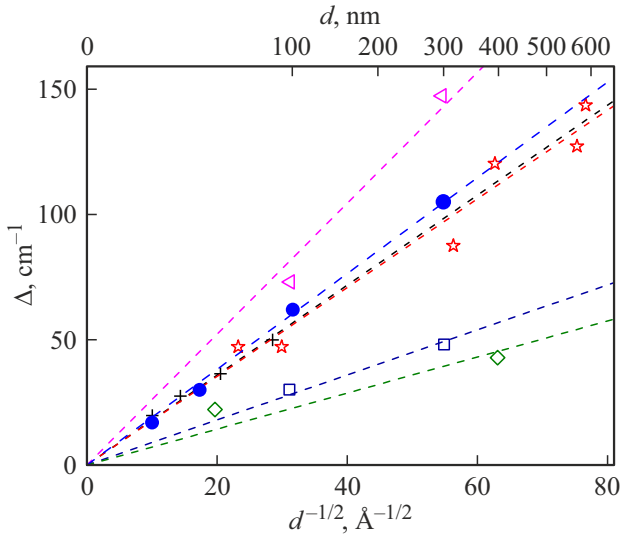

Figure 7. Dependence of SP dispersion curve splitting on the square root of width d of films for various film/substrate combinations: LiF/sapphire (crosses) [6], MgO/sapphire (circles) [the present work], LiF/MgO (stars) [15], ZnO/CaF_2 (triangles) [19], ZnO/LiF (squares) [19], AlN/sapphire (rhombs) [14]. Dashed lines denote linear approximation for each film/substrate pair.

The square root of film thickness d was chosen on the y-axis because in this case it is expected that experimental points on the curve shall lie on a straight line starting at the origin. The dashed line of the same color is the linear fit by function $\Delta = \alpha x$, where $x = \sqrt{d}$, α is the coefficient of proportionality. Blue circles fit well with the linear dependence. This supports the conclusion in [1] concerning the fact that SP dispersion branch splitting is proportional to the square root of transition layer thickness provided that there is resonance with the transition layer phonon.

Figure 7 shows similar dependences for various film/substrate combinations [6,14,15,19]. SP dispersion curve splitting was observed in all cases. Splitting in the ATR spectra was detected already for films having a thickness of about 10 nm, the most distinctive splitting was observed for the 27 nm films. The depth of both minima is significant only in the vicinity of the resonance, when moving away from the resonance, the spectrum approached the profile of a spectrum without film, and the line intensity decreases rapidly similarly to the results discussed in the present work. The presented data set explicitly supports the conclusions in [1].

4. Conclusion

Experimental results of the study of the substrate's SP dispersion curve splitting due to the resonance with the transition layer phonon are shown for the MgO films on sapphire surface. Conclusions made by V.M. Agranovich and A.G. Mal'shukov in their theoretical work [1], that laid the foundation for using the SP spectroscopy as a thin film examination method, are supported. In particular, it is shown that experimental splittings in agreement with the theoretical data are proportional to the square root of film thickness, i.e. they decrease not so fast as the thickness decreases. The effect is reliably detected on the ~ 30 nm films. It also occurs on the ~ 10 nm films, but is much weaker.

Acknowledgments

This study was carried out under state assignment № FFUU-2022-0003. The authors are grateful to the colleagues from the Institute of Inorganic Chemistry and Surfaces (Padova, Italy) for the provided samples of MgO nanofilms on sapphire.

Conflict of interest

The authors declare that they have no conflict of interest.

References

[1] V.M. Agranovich, A.G. Malshukov. Opt. Commun., **11** (2), 169 (1974). DOI: 10.1016/0030-4018(74)90211-9
[2] V.M. Agranovich. UFN, **115** (2), 199 (1975) (in Russian). DOI: 10.3367/UFNr.0115.197502b.0199.
[3] *Surface polaritons. Electromagnetic waves at surfaces and interfaces*, V.M. Agranovich and D.L. Mills eds, North-Holl. Publ. Co, Amsterdam, 1982.
[4] I.A. Dorofeyev, E.A. Vinogradov. Phys. Rep., **504**, 75 (2011). DOI: 10.1016/j.physrep.2011.03.004
[5] G.N. Zhizhin, O.I. Kapusta, M.A. Moskaleva, V.G. Nazin, V.A. Yakovlev. Sov. Phys. Usp., **18**, 927–928 (1975). DOI: 10.1070/PU1975v018n11ABEH005241.
[6] V.A. Yakovlev, V.G. Nazin, G.N. Zhizhin. Opt. Commun., **15** (2), 293 (1975). DOI: 10.1016/0030-4018(75)90306-5
[7] G.N. Zhizhin, M.A. Moskalyova, V.G. Nazin, V.A. Yakovlev. ZhETF, **72**, 687 (1977). (in Russian).
[8] V.A. Yakovlev, N.N. Novikova, E.A. Vinogradov, S.S. Ng, Z. Hassan, H. Abu Hassan. Phys. Lett. A, **373**, 2382 (2009). DOI: 10.1016/j.physleta.2009.04.051
[9] V.A. Yakovlev, N.N. Novikova, E.A. Vinogradov, S.S. Ng, Z. Hassan, H. Abu Hassan. J. Phys.: Conf. Ser., **210** (1), 012027 (2010), DOI: 10.1088/1742-6596/210/1/012027
[10] V.A. Yakovlev, N.N. Novikova, E.A. Vinogradov, G. Rossetto, A. Sartori, M. Bolzan. J. Nanoparticle Research, **13** (11), 5841 (2011). DOI: 10.1007/s11051-011-0280-8
[11] N.N. Novikova, E. Ol'shanskii, A.A. Teplov, D.C. Shaitura, V.A.Yakovlev. Phys. Sol. St., **54** (3), 573 (2012). DOI: 10.1134/S1063783412100332.
[12] N.N. Novikova, E.A. Vinogradov, V.A. Yakovlev, T.V. Malin, V.G. Mansurov, K.S. Zhuravlev. Surface and Coating Technology, **227**, 58 (2013). DOI: 10.1016/j.surfcoat.2013.02.037
[13] E.A. Vinogradov, N.N. Novikova, V.A. Yakovlev. Phys. Usp., **57** (6), 604b (2014). DOI: 10.3367/UFNe.0184.201406g.0653.
[14] N.N. Novikova, E.A. Vinogradov, V.A. Yakovlev, T.V. Malin, V.G. Mansurov, K.S. Zhuravlev. PSS(c), **12** (4–5), 439 (2015). DOI: 10.1002/pssc.201400177

[15] G.N. Zhizhin, E.A. Vinogradov, M.A. Moskalova, V.A. Yakovlev. Appl. Spectrosc. Rev., **18** (2), 171 (1983). DOI: 10.1080/05704928208055768
[16] D.S. Milakhin, T.V. Malin, V.G. Mansurov, A.S. Kozhukhov, N.N. Novikova, V.A. Yakovlev, K.S. Zhuravlev. FTP, **56** (8), 734 (2022) (in Russian). DOI: 10.61011/EOS.2024.08.60023.6792-24
[17] V.A. Yakovlev, N.N. Novikova, E.A. Vinogradov, G. Rossetto, A. Sartori, M. Bolzan. J. Nanopart. Res., **13** (11), 5841 (2011). DOI: 10.1007/s11051-011-0280-8
[18] S.S. Ng, S.C. Lee, S.K. Mohd Bakhori, Z. Hassan, H.A. Hassan, V.A. Yakovlev, N.N. Novikova, E.A. Vinogradov. Opt. Express, **18** (10), 10354 (2010). DOI: 10.1364/OE.18.010354
[19] N.N. Novikova, V.A. Yakovlev, E.A. Vinogradov, S.S. Ng, Z. Hassan, H. Abu Hassan. Appl. Surface Sci., **267**, 93 (2013). DOI: 10.1016/j.apsusc.2012.07.157
[20] A. Sartori, N. El Habra, M. Bolzan, G. Rossetto, S. Sitran, D. Barreca, A. Gasparotto, M. Casarin. Chem. Mater., **23** (5), 1113 (2013). DOI: 10.1021/cm1020788
[21] A. Otto. Z. Phys., **216**, 398 (1968). DOI: 10.1007/BF01391532
[22] G. Borstel, H.J. Falge, A. Otto. In: *Solid-State Physics. Springer Tracts in Modern Physics* (Springer, Berlin, Heidelberg, 1974), vol. 74, p. 107–148. DOI: 10.1007/BFb0041387
[23] A.S. Barker Jr. Phys. Rev., **132**, 1474 (1963). DOI: 10.1103/PhysRev.132.1474
[24] A. Mitsuishi, H. Yoshinaga, S. Fujita, Y. Suemoto. Jpn. J. Appl. Phys., **1**, 1 (1962). DOI: 10.1143/JJAP.1.1
[25] Y. Kumagai, H. Yokoi, H. Tampo, Y. Tabata, N. Kuroda. J. Phys. Soc. Jpn., 81, **1** (2012). DOI: 10.1143/JPSJ.81.024709
[26] L. Pauling, S.B. Hendkicks. J. Am. Chem. Soc., **47**, 781 (1925). DOI: 10.1021/ja01680a027
[27] R.E. Newnham, Y.M. de Haan. Zeitschrift für Kristallographie, **117** (2–3), 235 (1962). DOI: 10.1524/zkri.1962.117.2-3.235
[28] W. Theiß. Hard- and Software, SCOUT, Technical Manual [Electronic source]. URL: www.mtheiss.com
[29] M. Krüger, S. Hilbrich, M. Thönissen, D. Scheyen, W. Theiß, H. Lüth. Opt. Commun., **146**, 309 (1998). DOI: 10.1016/S0030-4018(97)00513-0.
[30] A.B. Kuzmenko. Rev. Sci. Instruments, **76**, 083108 (2005). DOI: 10.1063/1.1979470
[31] J. F. Scott, S. P. S. Porto. Phys. Rev., **161**, 903 (1967). DOI: 10.1103/PhysRev.161.903
[32] F. Gervais, B. Piriou. Phys. Rev. B, **11**, 3944 (1975). DOI:10.1103/PhysRevB.11.3944
[33] S.A. Klimin, A.B. Kuzmenko, M.A. Kashchenko, M.N. Popova. Phys. Rev. B, **93**, 054304 (2016). DOI: 10.1103/PhysRevB.93.054304
[34] F. Gervais. Opt. Commun., **22**, 116 (1977). DOI: 10.1016/0030-4018(77)90260-7
[35] E.A. Vinogradov, B.N. Mavrin, N.N. Novikova, V.A. Yakovlev. Physics-Uspekhi, **52** (3), 290 (2009). DOI: 10.3367/ufne.0179.200903l.0313/
[36] E.A. Vinogradov.Physics-Uspekhi, **63** (88), 775 (2020). DOI: 10.3367/UFNe.2020.01.038719.
[37] V.A. Yakovlev, N.N. Novikova, A.D. Molchanova, V.A. Tchernyshov, S.A. Klimin. FTT **66**, 981 (2024). (in Russian)
[38] J.R. Jasperse, A. Kahan, J.N. Plendl, S.S. Mitra. Phys. Rev. **146**, 526 (1966). DOI: 10.1103/PhysRev.146.526
[39] G. Andermann, E. Duesler. J. Opt. Soc. Am., **60** (1), 53 (1970). DOI: 10.1364/JOSA.60.000053
[40] P. Giura, L. Paulatto, F. He, R.P.S.M. Lobo, A. Bosak, E. Calandrini, L. Paolasini, D. Antonangeli. Phys. Rev. B, **99**, 220304 (2019). DOI: 10.1103/PhysRevB.99.220304
[41] A.M. Hofmeister, E. Keppel, A.K. Speck. Mon. Not. R. Astron. Soc., **345** (1), 16 (2003). DOI: 10.1046/j.1365-8711.2003.06899.x
[42] V.G. Tsirel'son, A.S. Avilov, Yu.A. Abramov, E.L. Belokoneva, R. Kitaneh, D. Feil. Acta Crystallographica, Section B: Structural Science, 54, 8 (1998). DOI: 10.1107/S0108768197008963
[43] H.J. Falge, A. Otto. Phys. Stat. Sol. (b), **56**, 523 (1973). DOI: 10.1002/pssb.2220560213

Translated by E.Ilinskaya